STEM CELLS®

EMBRYONIC STEM CELLS/INDUCED PLURIPOTENT STEM CELLS

Polycystin-2 Plays an Essential Role in Glucose Starvation-Induced Autophagy in Human Embryonic Stem Cell-Derived Cardiomyocytes

JUN LU ,[a,b] KENNETH R. BOHELER,[c] LIWEN JIANG,[d] CAMIE W. CHAN,[c] WAN WAI TSE,[e] WENDY KEUNG,[e] ELLEN NY POON,[c] RONALD A. LI,[e,f] XIAOQIANG YAO[a,b]

[a]School of Biomedical Sciences and Li Ka Shing Institute of Health Sciences, Faculty of Medicine, the Chinese University of Hong Kong, Hong Kong, People's Republic of China; [b]Shenzhen Research Institute, The Chinese University of Hong Kong, Shenzhen, People's Republic of China; [c]School of Biomedical Sciences, LKS Faculty of Medicine, The University of Hong Kong, Hong Kong, People's Republic of China; [d]Centre for Cell and Developmental Biology, State Key Laboratory of Agrobiotechnology, School of Life Sciences, The Chinese University of Hong Kong, Hong Kong, People's Republic of China; [e]Dr. Li Dak-Sum Research Centre, The University of Hong Kong Karolinska Institutet Collaboration in Regenerative Medicine, Hong – Kong, People's Republic of China; [f]Ming Wai Lau Centre for Reparative Medicine, Karolinska Institutet, Sweden

Correspondence: Xiaoqiang Yao, Ph.D., School of Biomedical Sciences, The Chinese University of Hong Kong, Shatin, Hong Kong SAR, People's Republic of China. Telephone: 852-39436877; e-mail: yao2068@cuhk.edu.hk

Received May 8, 2017; accepted for publication December 3, 2017; first published online in STEM CELLS *EXPRESS* December 22, 2017.

http://dx.doi.org/10.1002/stem.2764

Key Words. Autophagy • Po lycystin-2 • Human embryonic stem cell-derived cardiomyocytes • Glucose starvation • Ryanodine receptor

ABSTRACT

Autophagy is a process essential for cell survival under stress condition. The patients with autosomal dominant polycystic kidney disease, which is caused by polycystin-1 or polycystin-2 (PKD2) mutation, display cardiovascular abnormalities and dysregulation in autophagy. However, it is unclear whether PKD2 plays a role in autophagy. In the present study, we explored the functional role of PKD2 in autophagy and apoptosis in human embryonic stem cell-derived cardiomyocytes. HES2 hESC line-derived cardiomyocytes (HES2-CMs) were transduced with adenoviral-based *PKD2*-shRNAs (Ad-*PKD2*-shRNAs), and then cultured with normal or glucose-free medium for 3 hours. Autophagy was upregulated in HES2-CMs under glucose starvation, as indicated by increased microtubule-associated protein 1 light chain 3-II level in immunoblots and increased autophagosome and autolysosome formation. Knockdown of PKD2 reduced the autophagic flux and increased apoptosis under glucose starvation. In Ca^{2+} measurement, Ad-*PKD2*-shRNAs reduced caffeine-induced cytosolic Ca^{2+} rise. Co-immunoprecipitation and in situ proximity ligation assay demonstrated an increased physical interaction of PKD2 with ryanodine receptor 2 (RyR2) under glucose starvation condition. Furthermore, Ad-*PKD2*-shRNAs substantially attenuated the starvation-induced activation of AMP-activated protein kinase (AMPK) and inactivation of mammalian target of rapamycin (mTOR). The present study for the first time demonstrates that PKD2 functions to promote autophagy under glucose starvation, thereby protects cardiomyocytes from apoptotic cell death. The mechanism may involve PKD2 interaction with RyR2 to alter Ca^{2+} release from sarcoplasmic reticulum, consequently modulating the activity of AMPK and mTOR, resulting in alteration of autophagy and apoptosis. STEM CELLS *2018;36:501–513*

SIGNIFICANCE STATEMENT

Autosomal dominant polycystic kidney disease (ADPKD) caused by mutations in either polycystin-1 or polycystin-2 is often accompanied by cardiovascular problems. With the use of human embryonic stem cell-derived cardiomyocytes as model, this study shows an important functional role of polycystin-2 in promoting autophagy and reducing apoptotic death under glucose starvation. The mechanism involves polycystin-2 interaction with ryanodine receptor 2 to modulate calcium release from sarcoplasmic reticulum, consequently modulating the activity of AMP-activated protein kinase and mammalian target of rapamycin, resulting in alteration of autophagy and apoptosis in human embryonic stem cell-derived cardiomyocytes. This scheme may have important pathophysiological relevance in ADPKD and ischemic heart diseases.

INTRODUCTION

Autosomal dominant polycystic kidney disease (ADPKD) is a common hereditary disorder with an incidence of 1 in 400–1,000 individuals [1]. It is caused by loss-of function heterozygous mutations either in polycystin-1 (PKD1) or polycystin-2 (PKD2). The hallmark of ADPKD is the development of hundreds of microscopic fluid-filled cysts in the kidney, causing loss of normal renal tissue [1]. In addition, ADPKD patients develop cardiac diseases with more than 70% of the patients having hypertension and more than 90% of the patients exhibiting left ventricular hypertrophy at death [2, 3]. However, the mechanism of how PKD1 and PKD2 mutation could lead to cardiac disorders is incompletely understood.

Autophagy is a highly conserved process essential for cell survival under stress conditions including nutrient starvation, hypoxia, and intracellular stress [4]. Recent studies have suggested that suppression of autophagy could underlie disease progression in ADPKD [5, 6]. It is reported that PKD1 knockout impairs autophagic flux and increases apoptosis in kidney cells, which could be a contributing reason for cyst formation in ADPKD [5–7]. Furthermore, autophagy could serve to promote survival of cardiomyocytes by breaking down unnecessary and malfunctioned proteins at least under certain conditions such as glucose starvation and ischemia [8–10]. Cytosolic Ca^{2+} change, due to alteration in extracellular Ca^{2+} entry and/or intracellular store Ca^{2+} release, is an important regulator of autophagy [11, 12]. Ca^{2+} could act through multiple downstream targets including AMP-activated protein kinase (AMPK) and mammalian target of rapamycin (mTOR) to regulate autophagy [11, 12].

PKD2 is a 968 amino acid membrane protein with six transmembrane segments. It is a Ca^{2+}-permeable nonselective ion channel predominantly localized in endoplasmic/sarcoplasmic reticulum (ER/SR) [13]. A recent study suggested that the channel may be more permeable to Na^{+}/K^{+} than to Ca^{2+} [14]. PKD1 is a much bigger protein with ~4,300 amino acids and 11 transmembrane segments, with six of these transmembrane segments sharing sequence similarity with PKD2 [15, 16]. PKD1 itself is not an ion channel [15, 16]. Functionally, PKD1 binds to PKD2 to induce the translocation of PKD2 to the plasma membrane, where it serves as a Ca^{2+}-permeable ion channel [13, 15, 16]. PKD1 and PKD2 can form a complex via an interaction between their C-termini to modulate mechanosensitive Ca^{2+} response in renal cells [17].

Ryanodine receptor (RyR2) in cardiomyocytes is the major Ca^{2+} release channel located in the SR membrane. It is responsible for releasing the bulk of Ca^{2+} required for contraction. During heart beating, fast upstroke depolarization during the action potential activates extracellular Ca^{2+} influx via L-type Ca^{2+} channels located in the transverse tubules. This, in turn, activates sarcoplasmic RyR2 channels to release SR Ca^{2+}, consequently leading to cardiomyocyte contraction [18].

One report shows that, in cardiomyocytes, the C terminus of PKD2 binds to RyR2 in its open state, subsequent inhibiting Ca^{2+} release from SR and causing an elevation in store Ca^{2+} content. As a result of the elevated store Ca^{2+} content, the amount of SR Ca^{2+} release is increased during spontaneous Ca^{2+} oscillations and/or caffeine-induced Ca^{2+} transients [19]. In another report, the cardiomyocytes derived from heterozygous *PKD2*$^{+/-}$ mouse was found to exhibit an abnormal spontaneous Ca^{2+} oscillation and a reduced Ca^{2+} release in response to a RyR2 agonist caffeine [19, 20]. In zebrafish model of PKD2 knockout, PKD2 mutant hearts display impaired intracellular Ca^{2+} cycling and Ca^{2+} alternans [21]. These data demonstrate that PKD2 plays an important role in regulating RyR2-mediated intracellular Ca^{2+} release in the heart. Interestingly, cardiomyocytes with reduced RyR2 expression (*RyR2*$^{+/-}$) not only exhibit a reduced Ca^{2+} release, but also display a decreased autophagy, suggesting a linkage between RyR2-mediated Ca^{2+} release and autophagy [22]. However, up to the present there is still no report about the role of PKD2 in autophagy in cardiomyocytes.

Human embryonic stem cells (hESCs) and human-induced pluripotent stem cells (hiPSCs) provide an unlimited source of human cardiomyocytes for potential application in disease modeling, drug screening, and cell-based heart therapies. These hESC- or hiPSC-derived cardiomyocytes (hESC-CMs or hiPSC-CMs) are suggested to have many properties of authentic human cardiomyocytes [23]. In the present study, we used two types of hESC-CMs, HES2-CMs and H7-CMs, as models to investigate the potential role of PKD2 in autophagy. Our results demonstrated an important role of PKD2 in promoting autophagic flux and reducing apoptosis in human cardiomyocytes under glucose starvation.

Materials and Methods

Differentiation and Isolation of HES2-CMs and H7-CMs

Detailed methods about the differentiation and isolation of HES2-CMs and H7-CMs were described elsewhere [24]. In brief, HES2 cells from passage 40 to 80 were suspension-cultured to form embryoid bodies (EBs), and then differentiated to cardiomyocytes in culture media with addition of recombinant human bone morphogenetic protein 4 (BMP-4) and activin-A under a hypoxic condition of 5% O_2. At 8 days after cardiac differentiation, EBs were transferred to a normoxic environment and maintained in StemPro34 SFM (Invitrogen, NY) with ascorbic acid (50 μg/ml, Sigma, NY) medium for further characterization. HES2-CMs were isolated by digesting beating cardiospheres (30–40 days) with collagenase IV (1 mg/ml, Gibco, NY) at 37°C for 30 minutes, and then dissociated with Trypsin/EDTA (ethylenediaminetetraacetic acid, 0.05%, Life Technologies). In some experiments, human H7 ESCs maintained in Essential 8 Medium (Life Technologies) were differentiated to cardiomyocytes in RPMI/B27 (Invitrogen, NY) medium lacking insulin. Differentiation was induced using a modified confluent monolayer system by addition of 6 μM CHIR99021 (Selleckchem, Houston, a GSK3 inhibitor) from days 0 to 2 followed by addition of 10 μM IWR-1 (Enzo Life Sciences, NY, a WNT inhibitor) from days 3 to 5 in the absence of BMP-4 or activin-A. H7-CMs were isolated by digesting contracting monolayer with Trypsin/EDTA and maintained in RPMI/B27 medium with insulin. For glucose starvation experiments, glucose-free RPMI/B27 medium was used.

Adenoviral-Based Short Hairpin RNA

Recombinant adenovirus was generated using the AdEasy system [25]. The sequences of two short hairpin RNA (shRNA) used were 5′-GCAGAGATTGAGGAAGCTAAT-3′ and 5′-CCAGGA CTTGAGAGATGAAAT-3′, respectively. Two shRNA constructs against human PKD2 were synthesized, annealed, and subcloned into pAdTrack-U6. Adenoviral recombinants were generated in *Escherichia coli* strain BJ5183 with an adenoviral backbone plasmid, pAdEasy-1. Positive recombinants were linearized by *Pac*I digestion and transfected into HEK-293A cells for virus packaging. The medium and cells were collected until the cytopathic effect was apparent. Recombinant adenoviruses were purified by AdenoPACK 20 Maxispin column (Satorious, Germany) and concentrated by VIVA-SPIN 20 concentrator (100 kDa cut-off, Satorious, Germany). Scrambled shRNA in adenoviral vector (Ad-SCR-shRNA) was used as control. HES2-CMs or H7-CMs were transduced with adenoviral-based constructs.

After 96 hours, cells were ready for experiments. All subsequent experiments were performed when the cell confluence was about 70%. Ad-mCherry-GFP-LC3 was a generous gift from Dr. Huang Y, The Chinese University of Hong Kong.

Lentiviral-Based Wild-Type PKD2 and RyR2 shRNAs

Human PKD2 (NM_000297) was inserted into lenti-vector to yield a recombinant lentiviral construct pLVX-EF1α-*PKD2*-Puro. HES2-CMs were transduced with pLVX-EF1α-*PKD2*-Puro at a MOI of 3. The cells were further subjected to puromycin selection. For the controls, hESC2-CMs were transduced with pLVX- EF1α-BLANK-Puro. For knockdown experiments, The GV298 vector carried *RyR2*-shRNA1 (5′-CATAATACAAGGTC-TAATT-3′) and *RyR2*-shRNA2 (5′-CAACAACTACTGGGACAAA-3′) together with a scrambled shRNA (SCR-shRNA) were purchased from GeneChem CO, Ltd (Shanghai, People's Republic of China). HES2-CMs were transduced with *RyR2*-shRNAs and SCR-shRNA individually followed by puromycin selection.

Short Interfering RNA

Short interfering RNAs (siRNAs) were synthesized by Dharmacon. The ablation of Atg5 was performed by transfection of the HES2-CMs with *Atg5*-siRNA: 5′-GUCCAUCUAAGGAUGCAA UTT-3′. Scrambled siRNA was used as control. HES2-CMs were transfected at 70% confluence using Lipofectamine RNAiMAX Reagent according to the manufacturer's protocol. After 48 hours, HES2-CMs were ready for experiments.

Cell Apoptosis and Protein Interaction Experiment

The experiments were performed using In Situ Cell Death Detection kit (Sigma) following the manufacture's instruction. Briefly, HES2-CMs were fixed with 4% paraformaldehyde (PFA) and permeabilized with 0.1% Triton X-100. After wash with PBS, the cells were incubated with terminal deoxynucleotidyl transferase dUTP nick end labeling (TUNEL) reaction mixture for 1 hour at 37°C in a humidified atmosphere in the dark. Cell nuclei are counterstained with 4′,6-diamidino-2-phenylindole (DAPI). Samples were examined under FV1000 confocal microscope at the excitation wavelength at 488 nm and detection wavelength of 515–565 nm (green).

Proximity Ligation Assay

Protein interactions were detected by Duolink In Situ reagents (Sigma) according to the supplier's protocol. Briefly, HES2-CMs on slides were fixed with 4% PFA and permeabilized with 0.1% Triton X-100. The samples were incubated with anti-PKD2 (1:50) and anti-RyR2 (1:50) antibodies at 4°C overnight. After incubation with PLA probe solution, ligation and amplification reactions were performed. The slides were mounted using Duolink In Situ Mounting Medium with DAPI, and analyzed by FV1000 confocal microscope.

Immunoblotting and Co-Immunoprecipitation

For immunoblotting experiments, HES2-CMs or H7-CMs lysates prepared in RIPA lysis buffer were resolved on SDS/PAGE gel and were blotted onto a polyvinylidene difluoride (PVDF) membrane. The protein concentration was measured by using the DC protein assay (Bio-Rad). For co-immunoprecipitation, 200 μg of HES2-CMs lysate was immunoprecipitated with 2 μg of anti-PKD2 antibody or anti-RyR2 antibody with protein G Agarose beads (Sigma) at 4°C overnight. Negative controls were mouse preimmune IgG (CST) or rabbit preimmune IgG (Proteintech). The PVDF membrane was blocked with 5% BSA in TBS for 1 hour, followed by incubation with primary antibodies: LC3 (1:1,000 dilution, NovusBio), PKD2 (1:500 dilution, Santa Cruz Biotechnology), caspase-3(1:1,000 dilution, CST), phospho-mTOR (1:1,000 dilution, CST), mTOR (1:1,000 dilution, CST), phospho-AMPK (1:1,000 dilution, CST), AMPK (1:1,000 dilution, CST), RyR2 (1:1,000 dilution, Thermo Fisher), β-actin (1:3,000 dilution, Santa Cruz Biotechnology), and β-tubulin (1:1,000 dilution, Santa Cruz Biotechnology). After incubation with appropriate secondary antibodies, immunodetection was accomplished via using horseradish peroxidase-conjugated secondary antibody and the enhanced chemiluminescence detection system.

Ca^{2+} Measurements

HES2-CMs were loaded with Fura-2/AM (5 μM, Invitrogen) or Fluo-4/AM (5 μM, Invitrogen) for 30 minutes in dark at 37°C. Fura-2 fluorescence signals was measured by dual excitation wavelength at 340 nm and 380 nm, and the emitted light signal was read at 510 nm. F340/F380 was calculated and acquired with MetaFluor imaging software (Molecular Devices). Fluo-4 was excited at 488 nm line and captured at wavelengths 505–530 nm. Data acquisition was performed using a confocal microscope (Olympus FV1000). Ca^{2+} imaging experiments were performed in Tyrode's solution containing in mM: NaCl 140, KCl 5.4, $CaCl_2$ 1.8, $MgCl_2$ 1, glucose 10, HEPES 10, adjusted to pH 7.40 with NaOH. Some experiments were carried out in a Ca^{2+}-free Tyrode's solution, which contained in mM: NaCl 140, KCl 5.4, EGTA 1, $MgCl_2$ 1, glucose 10, HEPES 10, adjusted to pH 7.40 with NaOH. All experiments were performed at 37°C or room temperature. For Fura-2, change in cytosolic Ca^{2+} was displayed as the change in 340/380 fluorescent ratio (Δ340/380). Ca^{2+} oscillations were measured based on Fluo-4 fluorescence. The frequency of Ca^{2+} oscillations was determined by MATHLAB software. The amplitude of Ca^{2+} oscillations was displayed as a ratio of maximal fluorescence increase relative to the basal intensity (F1/F0) and the data was analyzed by MetaFluor imaging software. The area under curve (AUC) of Ca^{2+} oscillations was analyzed by Origin7.0 software. The accumulated area under curve (AAUC) of Ca^{2+} oscillations was quantified the AUC in 1 minute. AUC and AAUC were presented as fold changes relative to control group.

Reagents

To inhibit autophagosome-lysosome fusion, HES2-CMs or H7-CMs were treated with 50 nM Bafilomycin A1 (Sigma) for 3 hours. To activate or block RyR2, 5 mM Caffeine (Sigma) or 20 μM ryanodine (Calbiochem) was applied individually. To activate β-adrenergic receptors, 10 μM isoprenaline (Sigma) was added. To visualize cell boundary, Alexa Fluor 546 Phalloidin (ThermoFisher) was used. Pluronic acid F-127, EGTA, glucose, $CaCl_2$, KCl, $MgCl_2$, and Hepes were purchased from Sigma.

Statistical Analysis

The experimental results were expressed as mean ± SEM. Statistical significance between groups of 2 were conducted with Student's *t* test. Groups of 3 or more were analyzed with one-way analysis of variance (ANOVA) following Bonferroni post hoc test. Statistical analyses were performed with the

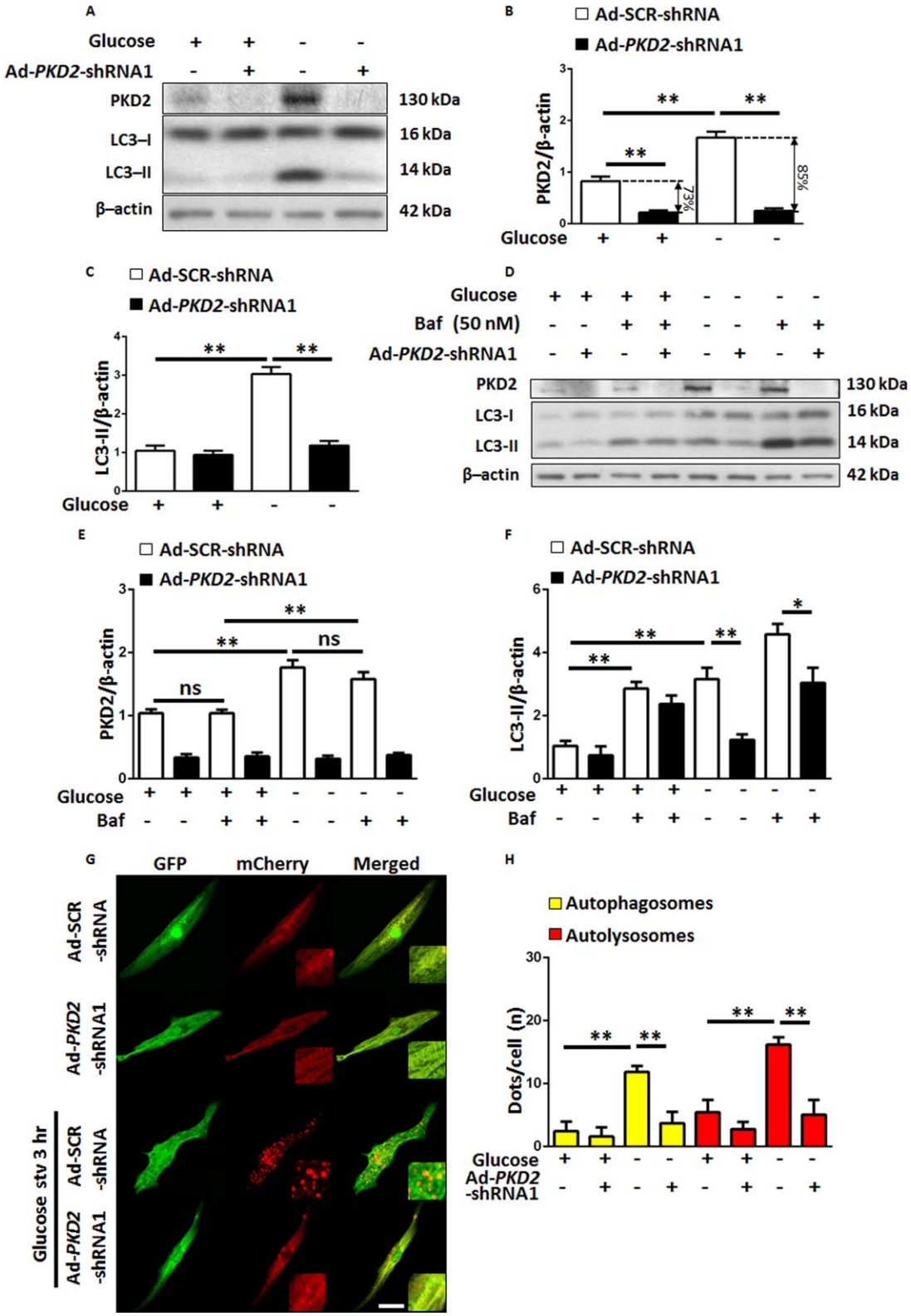

Figure 1. PKD2 knockdown reduced autophagic flux in HES2 hESC line-derived cardiomyocytes (HES2-CMs) under glucose starvation. HES2-CMs were transduced with Ad-SCR-shRNA or Ad-*PKD2*-shRNA1 for 96 hours, followed by culture with normal or glucose-free medium (glucose stv) for 3 hours. **(A–C)**: Representative immunoblots (A) of PKD2 and LC3 protein levels together with quantification (B, C). **(D–F)**: HES2-CMs were treated with or without Baf (50 nM) for 3 hours. Shown are representative immunoblots (D) of PKD2 and LC3 protein level together with quantification (E, F). **(G, H)**: HES2-CMs with or without PKD2 knockdown were transduced with Ad-mCherry-GFP-LC3 for 48 hours, followed by culture with normal or glucose-free medium for 3 hours. Shown are representative images of GFP and mCherry dots (G) together with quantification (H) of autophagosomes and autolysosomes. Values in data summary are mean ± SEM ($n = 4–5$ experiments). *, $p < .05$; **, $p < .01$, ns = not significant. Scale bar, 20 μm. Abbreviations: Ad-*PKD2*-shRNAs, adenoviral-based *PKD2*-shRNAs; Ad-SCR-shRNA, scrambled shRNA in adenoviral vector; Baf, bafilomycin A1; GFP, green fluorescent protein; glucose stv, glucose starvation; LC3-II, light chain 3-II; PKD2, polycystin-2.

use of Prisms 6.0 software (GraphPad Software Inc., La Jolla, CA). $p < .05$ was considered statistically significant.

Results

PKD2 Knockdown Reduced Autophagic Flux in HES2-CMs Under Glucose Starvation Condition

HES2-CMs were subjected to glucose starvation for 3 hours to stimulate autophagy. As expected, glucose starvation caused an accumulation of microtubule-associated protein 1 light chain 3-II (LC3-II) (Fig. 1A, 1C), which is a commonly used index for autophagy [26, 27]. Interestingly, glucose starvation also increased the expression of PKD2 proteins (Fig. 1A, 1B). To evaluate the role of PKD2 in autophagy, HES2-CMs were transduced with two adenoviral-based shRNAs, Ad-*PKD2*-shRNA1, and Ad-*PKD2*-shRNA2. Compared with Ad-SCR-shRNA, both Ad-*PKD2*-shRNA1 (Fig. 1A, 1B) and Ad-*PKD2*-shRNA2 (Supporting Information Fig. S1A, S1B) could effectively knock down the expression of PKD2 proteins by $\geq$80% in HES2-CMs with or without glucose starvation. Importantly, both Ad-*PKD2*-shRNA1 (Fig. 1A, 1C) and Ad-*PKD2*-shRNA2 (Supporting Information Fig. S1A, S1C) reduced the LC3-II accumulation under glucose starvation. A reduced LC3-II level could be explained by a decrease in autophagic induction or an increase in autolysosomal degradation. We used bafilomycin A1 to inhibit autolysosomal degradation. In the presence of 50 nM bafilomycin A1, both Ad-*PKD2*-shRNA1 (Fig. 1D, 1F) and Ad-*PKD2*-shRNA2 (Supporting Information Fig. S1F, S1G) still markedly reduced the LC3-II accumulation under starvation, suggesting that PKD2 promoted the autophagic flux independent of autolysosomal degradation. In addition, in the presence of 50 nM bafilomycin A1, glucose starvation still increased the expression of PKD2 proteins (Fig. 1D, 1E).

To further examine the effect of PKD2 on autophagic flux, HES2-CMs were transduced with the tandem reporter Ad-mCherry-GFP-LC3 [28], which labels autophagosome with dual red and green fluorescence and autolysosome with red only (Fig. 1G). The results confirmed that glucose starvation increased the number of autophagosome (yellow dots in merged pictures in Fig. 1G) and autolysosome (free red dots in merged pictures in Fig. 1G; Fig. 1G, 1H). Ad-*PKD2*-shRNA1 reduced the formation of autophagosome and autolysosome under glucose starvation (Fig. 1G, 1H), further confirming the role of PKD2 in promoting autophagic flux under glucose starvation condition.

Effect of PKD2 Knockdown on LC3-II Level in HES2-CMs Under Different Glucose Concentrations

HES2-CMs were exposed to different concentrations of glucose, ranging from 11 mM to 0 mM, for 3 hours. 11 mM glucose was chosen because HES2-CMs were differentiated under such a glucose concentration and because this concentration of glucose was commonly used to culture cardiomyocytes in other studies [29–31]. 5.5 mM glucose corresponded to fasting blood glucose level [32], while 1.4 mM and 0 mM glucose represented different degrees of glucose starvation. As expected, glucose starvation with 1.4 mM or 0 mM glucose increased the LC3-II levels (Fig. 2). Intriguingly, PKD2 knockdown with Ad-*PKD2*-shRNA1 reduced the LC3-II accumulation not only in HES2-CMs under 1.4 mM and 0 mM glucose

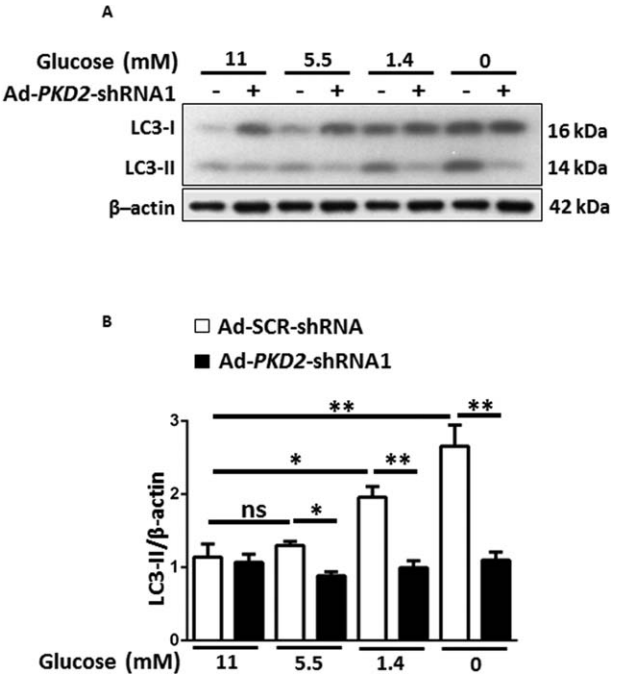

Figure 2. Polycystin-2 (PKD2) knockdown modulated autophagy at normal fasting blood glucose level in HES2 hESC line-derived cardiomyocytes (HES2-CMs). HES2-CMs were transduced with Ad-SCR-shRNA or Ad-*PKD2*-shRNA1 for 96 hours, followed by culture in RPMI/B27 medium with indicated doses of glucose for 3 hours. Shown are representative immunoblots **(A)** and quantification **(B)** of LC3 protein levels. Values in data summary are mean ± SEM ($n = 4$ experiments). *, $p < .05$; **, $p < .01$, ns = not significant. Abbreviations: Ad-*PKD2*-shRNAs, adenoviral-based *PKD2*-shRNAs; LC3-II, light chain 3-II; Ad-SCR-shRNA, scrambled shRNA in adenoviral vector.

(Fig. 2), but also in HES2-CMs under 5.5 mM glucose (Fig. 2), suggesting that PKD2 knockdown could modulate autophagy at normal fasting blood glucose level.

Overexpression of PKD2 Promoted Autophagic Flux in HES2-CMs

The effect of PKD2 overexpression on autophagy was examined (Fig. 3). As a validation, PKD2 overexpression indeed increased the PKD2 protein level (Fig. 3A, 3B). Importantly, PKD2 overexpression promoted autophagic flux as indicated by increase of LC3-II accumulation in HES2-CMs with or without glucose starvation (Fig. 3C, 3D). This effect persisted in the presence of 50 nM bafilomycin A1 at least under nonstarvation condition (Fig. 3C, 3D). PKD2 overexpression also increased the formation of autophagosome and autolysosome at least under basal nonstarvation condition in the tandem reporter Ad-mCherry-GFP-LC3 assay (Fig. 3E, 3F).

PKD2 Knockdown Promoted Apoptosis in HES2-CMs Under Glucose Starvation

The possible role of PKD2 in glucose starvation-induced apoptotic cell death in HES2-CMs was investigated using TUNEL and caspase 3 assays. In TUNEL assay, compared with Ad-SCR-shRNA, Ad-*PKD2*-shRNA1 (Fig. 4A, 4B), and Ad-*PKD2*-shRNA2 (Supporting Information Fig. S2A, S2B) increased the percentage of TUNEL-positive apoptotic cells under glucose starvation. In caspase 3 assay, treatment with Ad-*PKD2*-shRNA1

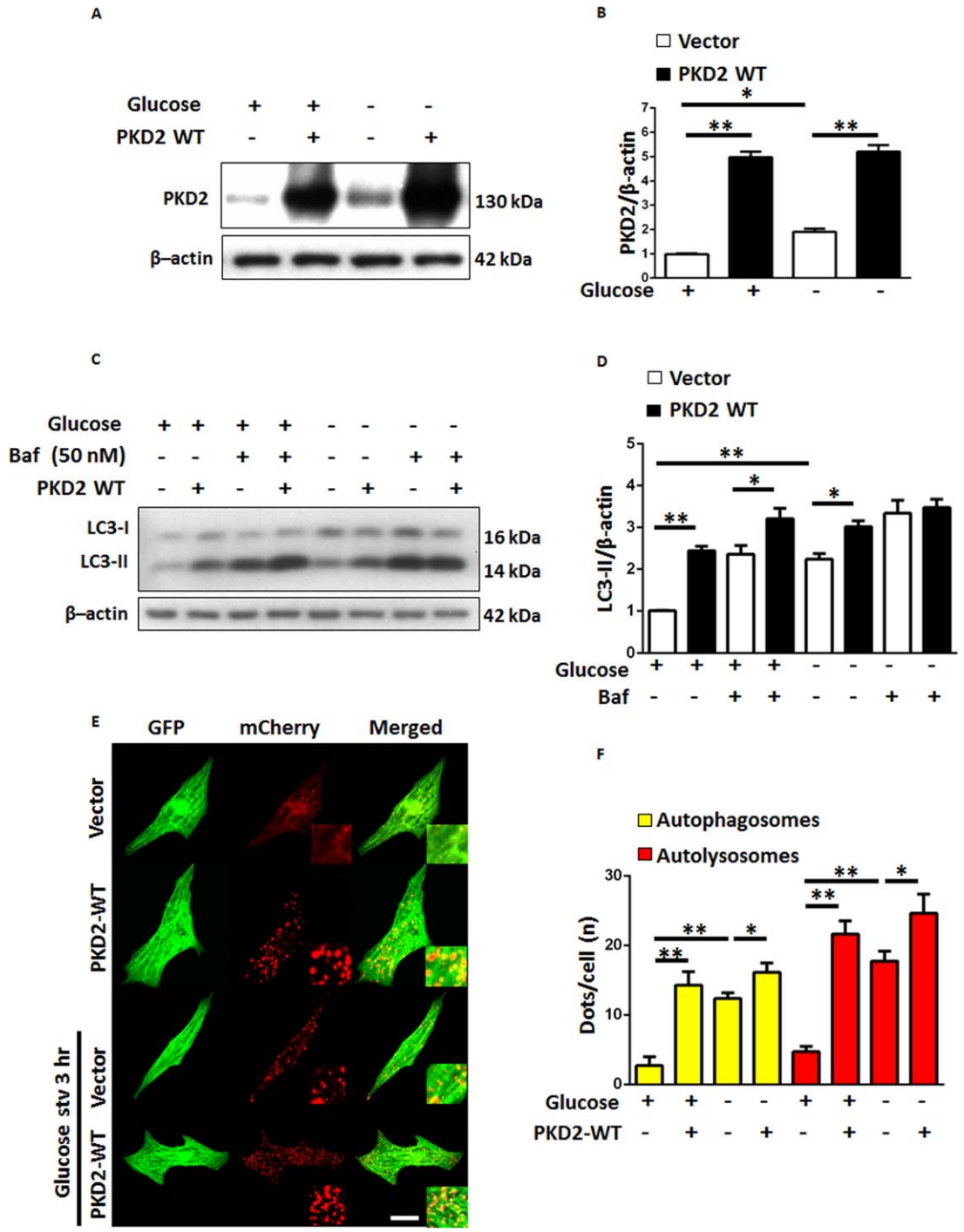

Figure 3. PKD2 overexpression promoted autophagic flux in HES2 hESC line-derived cardiomyocytes (HES2-CMs) under glucose starvation. HES2-CMs were transduced with plvx-puro-vector (Vector) or plvx-puro-*PKD2* (PKD2 WT) for 96 hours, followed by culture with normal or glucose-free medium for 3 hours. **(A, B)**: Representative immunoblots (A) of PKD2 protein levels together with quantification (B). **(C, D)**: HES2-CMs were treated with or without Baf (50 nM) for 3 hours. Shown are representative immunoblots (C) of LC3 protein level together with quantification (D). **(E, F)**: HES2-CMs with or without PKD2 overexpression were transduced with Ad-mCherry-GFP-LC3 for 48 hours, followed by culture with normal or glucose-free medium for 3 hours. Shown are representative images of GFP and mCherry dots (E) together with quantification (F) of autophagosomes and autolysosomes. Values in data summary are mean ± SEM ($n = 5$ experiments). *, $p < .05$; **, $p < .01$. Scale bar, 20 μm. Abbreviations: Baf, bafilomycin A1; GFP, green fluorescent protein; glucose stv, glucose starvation; LC3-II, light chain 3-II; PKD2, polycystin-2;

(Fig. 4C, 4D) and Ad-*PKD2*-shRNA2 (Supporting Information Fig. S2C, S2D) activated caspase-3, as indicated by an increased level of cleaved caspase-3 in Western blots (active form, 17 kDa). Together, these data suggest that PKD2 protects against apoptotic cell death of HES2-CMs under glucose starvation.

Next, we sought to confirm whether autophagy could indeed serve to protect HES2-CMs from starvation-induced

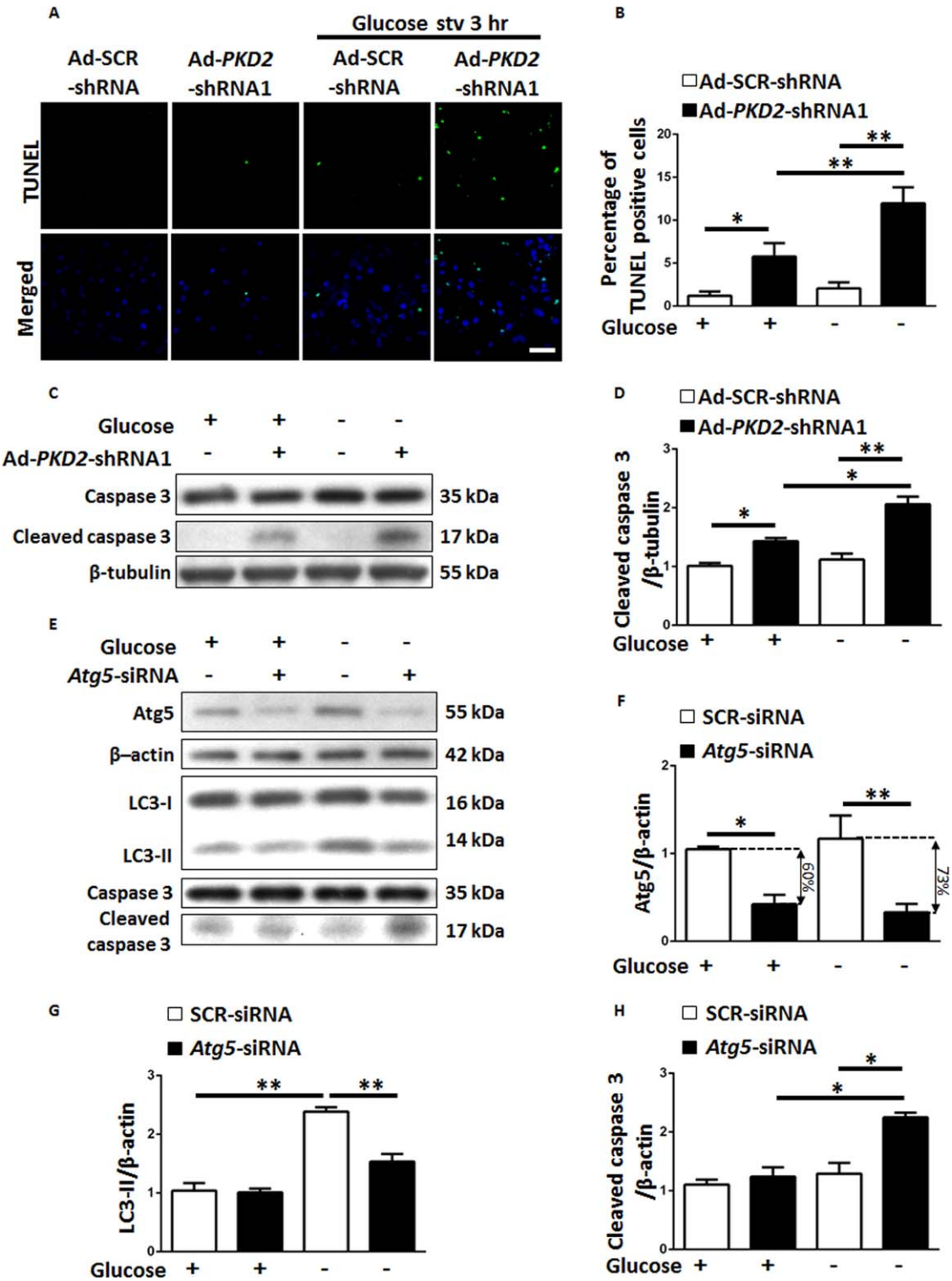

Figure 4. PKD2 knockdown promoted apoptosis in HES2 hESC line-derived cardiomyocytes (HES2-CMs) under glucose starvation. HES2-CMs were transduced with Ad-SCR-shRNA or Ad-*PKD2*-shRNA1 for 96 hours, followed by culture with normal or glucose-free medium for 3 hours. **(A, B)**: Representative pictures (A) and summary data (B) of TUNEL-positive cells. **(C, D)**: Representative immunoblots (C) and summary data (D) of caspase 3 and cleaved caspase 3 protein levels. HES2-CMs were transfected with si-SCR or si-Atg5 for 48 hours, followed by culture with normal or glucose-free medium for 3 hours. Shown are representative immunoblots **(E)** and quantification (**F–H**) of Atg5, LC3, caspase 3, and cleaved caspase 3 protein levels. Values in data summary are mean ± SEM ($n = 4$ experiments). *, $p < .05$; **, $p < .01$. Scale bar, 50 μm. Abbreviations: Ad-*PKD2*-shRNAs, adenoviral-based *PKD2*-shRNAs; Ad-SCR-shRNA, scrambled shRNA in adenoviral vector; glucose stv, glucose starvation; LC3-II, light chain 3-II; PKD2, polycystin-2; SCR-siRNA, scrambled siRNA.

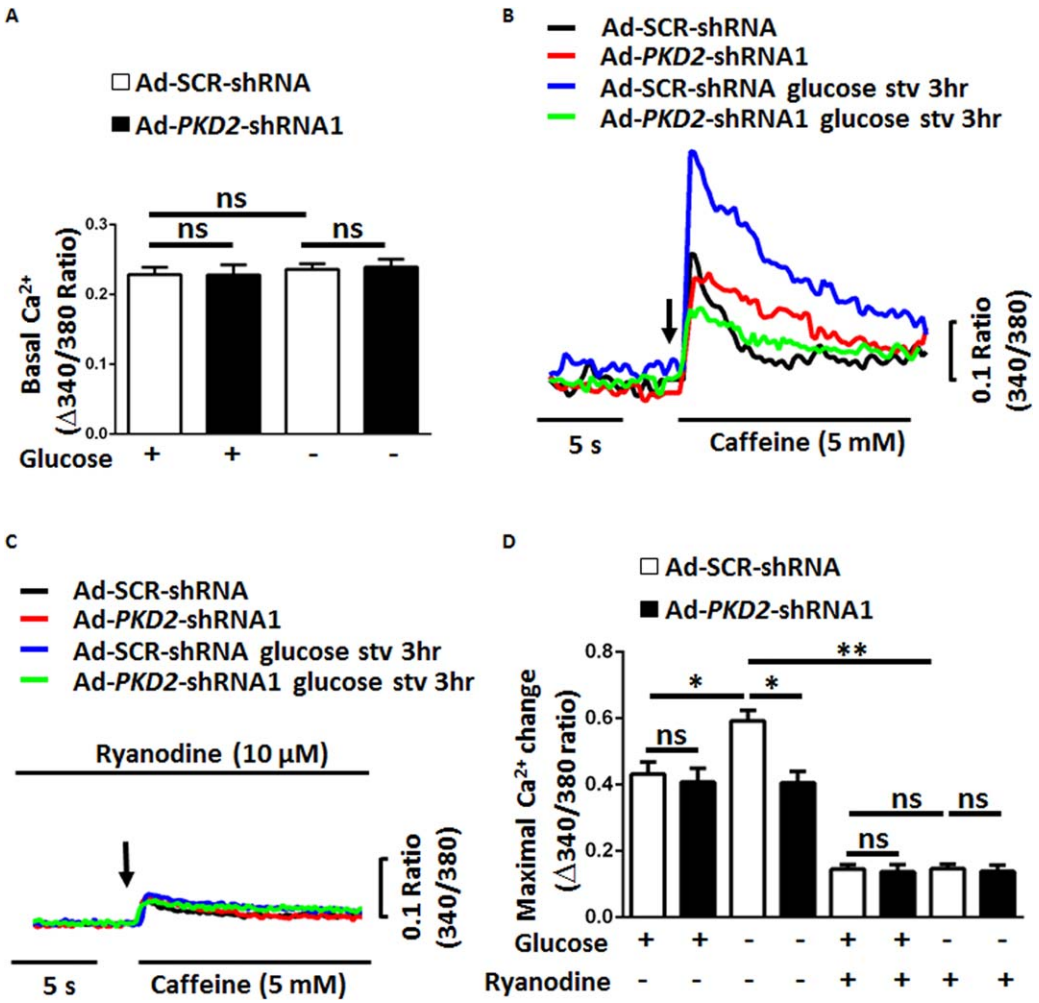

Figure 5. PKD2 knockdown reduced the caffeine-induced store Ca^{2+} release in HES2-CMs under glucose starvation. HES2-CMs were transduced with Ad-SCR-shRNA or Ad-*PKD2*-shRNA1 for 96 hours, followed by culture with normal or glucose-free medium for 3 hours. The cells were loaded with Fura-2/AM. **(A)**: Basal cytosolic Ca^{2+} level was not altered by Ad-*PKD2*-shRNA1 infection. **(B–D)**: Representative traces of Ca^{2+} transients elicited by 5 mM caffeine in the absence (B) and presence of 10 μM ryanodine (C) together with quantification (D) of maximal change of Ca^{2+} in response to 5 mM caffeine. Values in data summary are mean ± SEM ($n = 5$ experiments). *, $p < .05$; **, $p < .01$, ns = not significant. Abbreviations: Ad-*PKD2*-shRNAs, adenoviral-based *PKD2*-shRNAs; Ad-SCR-shRNA, scrambled shRNA in adenoviral vector; glucose stv, glucose starvation.

apoptosis. Atg5 is an E3 ubiquitin ligase essential for autophagosome elongation, which is a key step in autophagy [27]. *Atg5*-siRNA has been commonly used to disrupt autophagic flux [27]. As expected, *Atg5*-siRNA treatment disrupted autophagy, as indicated by its suppressing effect on LC3-II accumulation under starvation (Fig. 4E, 4G). Importantly, *Atg5*-siRNA treatment increased the starvation-induced apoptosis, as indicated by the increased level of cleaved caspase-3 under starvation (Fig. 4E, 4H). These results support that autophagy has a cytoprotective role in HES2-CMs under glucose starvation.

PKD2 Modulated RyR2-Mediated Ca^{2+} Release from SR in HES2-CMs

The role of PKD2 in modulating Ca^{2+} signaling of HES2-CMs was examined. Knockdown of PKD2 with Ad-*PKD2*-shRNA1 had no effect on basal cytosolic Ca^{2+} level in HES2-CMs under both normal and glucose starvation conditions (Fig. 5A). We next used a RyR agonist caffeine to examine RyR-mediated store Ca^{2+} release. The cells were bathed in a Ca^{2+}-free physiological saline containing 1 mM EGTA. Glucose starvation was found to increase the magnitude of caffeine (5 mM)-induced Ca^{2+} release from SR (Fig. 5B, 5D), reflecting an increased store Ca^{2+} content under glucose starvation [33]. Importantly, knockdown of PKD2 with Ad-*PKD2*-shRNA1 suppressed the caffeine-induced Ca^{2+} release under the glucose starvation (Fig. 5B, 5D). As a control, the caffeine-induced store Ca^{2+} release could be inhibited by a selective RyR antagonist ryanodine at 10 μM, confirming the involvement of RyR in the caffeine-induced cytosolic Ca^{2+} rise (Fig. 5C, 5D).

We explored the role of PKD2 in spontaneous cytosolic Ca^{2+} oscillations and isoprenaline-induced cytosolic Ca^{2+} response. The cells were bathed in normal Ca^{2+}-containing physiological saline at 37°C. Cytosolic Ca^{2+} oscillations were compared based on four indexes, frequency, amplitude, AUC, and AAUC (Supporting Information Fig. S3). Glucose starvation had no effect on the frequency (Supporting Information Fig.

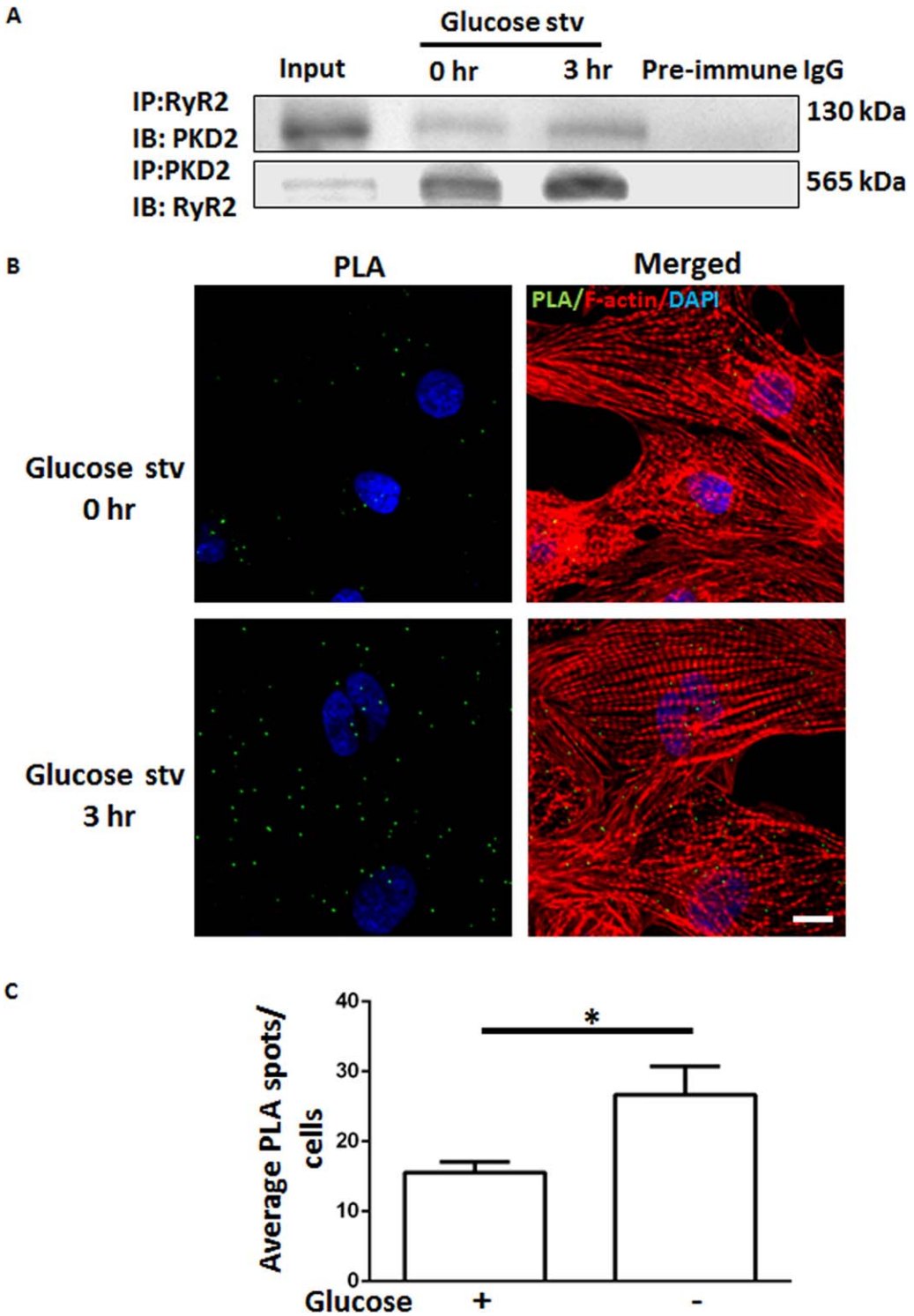

Figure 6. PKD2 interaction with RyR2. **(A)**: Representative images of co-immunoprecipitation of PKD2 with RyR2 from lysates of HES2-CMs with or without glucose starvation for 3 hours. **(B, C)**: Representative images (B) and data summary (C) of PKD2/RyR2 interaction in PLA. Values in data summary are mean ± SEM ($n = 4$ experiments). *, $p < .05$. Scale bar, 10 μm. Abbreviations: glucose stv, glucose starvation; PKD2, polycystin-2; PLA, proximity ligation assays; RyR2, ryanodine receptor 2.

S3B) but increased the amplitude and AUC of spontaneous Ca^{2+} oscillations (Supporting Information Fig. S3C, S3D). AAUC, which summarized the frequency and AUC, also increased under the glucose starvation (Supporting Information Fig. S3E). These results agree with the notion of an increased store Ca^{2+} content under glucose starvation [33]. Application of a β-adrenergic agonist isoprenaline at 10 μM increased the frequency of cytosolic Ca^{2+} oscillations in HES2-CMs under both normal and glucose starvation conditions (Supporting Information Fig. S3A, S3B). Importantly, knockdown of PKD2 with Ad-*PKD2*-shRNA1

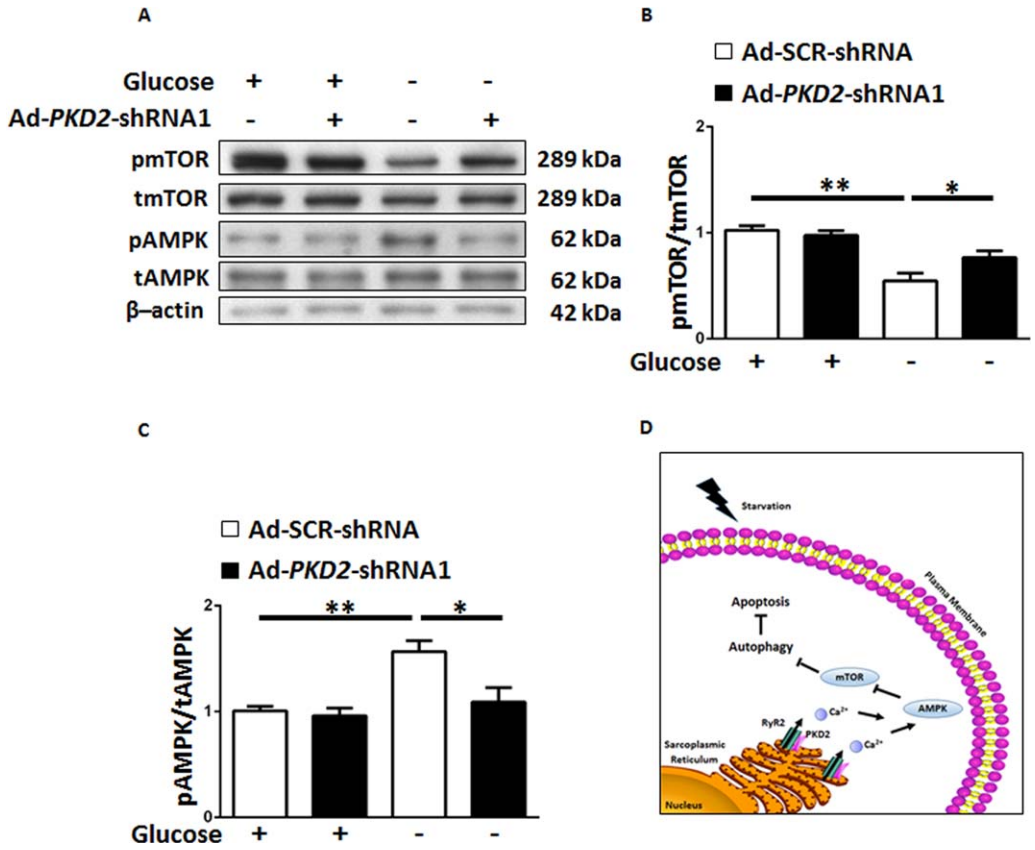

Figure 7. Downstream targets of PKD2-RyR2-mediated Ca^{2+} signaling were AMPK and mTOR. HES2-CMs were transduced with Ad-SCR-shRNA or Ad-*PKD2*-shRNA1 for 96 hours, followed by culture with normal or glucose-free medium for 3 hours. Shown are representative immunoblots **(A)** of pmTOR, tmTOR, pAMPK, and tAMPK protein levels together with quantification **(B, C)**. **(D)**: Schematic illustration showing that PKD2 interaction with RyR2 modulates Ca^{2+} release from SR, consequently regulating the activity of AMPK and mTOR, resulting in alteration of autophagy and apoptosis in HES2-CMs. Values in data summary are mean ± SEM ($n = 5$ experiments). *, $p < .05$; **, $p < .01$. Abbreviations: Ad-*PKD2*-shRNAs, adenoviral-based *PKD2*-shRNAs; Ad-SCR-shRNA, scrambled shRNA in adenoviral vector; pAMPK, phosphorylated AMPK; pmTOR, phosphorylated mTOR; tAMPK, total AMPK; tmTOR, total mTOR.

(Supporting Information Fig. S3A, S3C, S3D) and Ad-*PKD2*-shRNA2 (Supporting Information Fig. S4A, S4C, S4D) greatly reduced the amplitude and AUC of spontaneous and isoprenaline-stimulated cytosolic Ca^{2+} transients. Ad-*PKD2*-shRNA1 (Supporting Information Fig. S3A, S3B) and Ad-*PKD2*-shRNA2 (Supporting Information Fig. S4A, S4B) also reduced the frequency of isoprenaline-stimulated cytosolic Ca^{2+} transients. Furthermore, PKD2 knockdown drastically reduced the AAUC, which reflected the overall amount of Ca^{2+} release, during spontaneous cytosolic Ca^{2+} oscillations and isoprenaline-induced cytosolic Ca^{2+} oscillations (Supporting Information Figs. S3E, S4E). As a control, we found that the spontaneous cytosolic Ca^{2+} oscillations could be inhibited by ryanodine at 10 μM, confirming the involvement of RyR in the process (Supporting Information Figs. S3F, S3G, S4F, S4G).

Physical Interaction of PKD2 with RyR2 in HES2-CMs

Co-immunoprecipitation and proximity ligation assays (PLA) were used to examine the physical interaction of PKD2 with RyR2. In co-immunoprecipitation experiments, an anti-RyR2 antibody could pull down PKD2 in the protein lysates freshly prepared from HES2-CMs (Fig. 6A). Furthermore, an anti-PKD2 antibody could reciprocally pull down RyR2 (Fig. 6A). Interestingly, glucose starvation increased the amount of PKD2-RyR2 complex (Fig. 6A). In control experiments, in which immunoprecipitation was performed with the IgG purified from preimmune serum, no band was observed (Fig. 6A).

In situ proximity ligation assay was used to further confirm the physical interaction of PKD2 with RyR2 at subcellular level. In these experiments, the site of PKD2/RyR2 interaction could be visualized as a distinct fluorescent spot under fluorescence microscopy. In agreement with co-immunoprecipitation results, glucose starvation increased the number of fluorescence spots in the cells (Fig. 6B, 6C). Taken together, PKD2/RyR2 interaction occurred in HES2-CMs and was enhanced under glucose starvation.

RyR2 Knockdown Reduced Autophagy in HES2-CMs Under Glucose Starvation Condition

Previously, cardiomyocytes with reduced RyR2 expression ($RyR2^{+/-}$ mice) have been shown to have a decreased autophagy [22]. Here we attempted to verify this finding in our system. Two lentiviral-based *RyR2*-shRNAs were constructed, both of which could effectively knock down the expression of RyR2 protein expression (Supporting Information Fig. S5A, S5B). Knockdown of RyR2 expression by each of the two RyR2-shRNAs reduced the starvation-induced LC3-II accumulation (Supporting Information Fig. S5C, S5D). Furthermore,

functional inhibition of RyR2 by 20 μM ryanodine also reduced the starvation-induced LC3-II accumulation (Supporting Information Fig. S5E, S5F). These data support the role of RyR2 in autophagy.

Downstream Targets of PKD2-RyR2-Mediated Ca^{2+} Signaling Were AMPK and mTOR

We explored possible downstream targets of PKD2-RyR2-mediated Ca^{2+} signaling. Ca^{2+} may act through AMPK and mTOR to regulate autophagy [11, 12]. In agreement with this notion, under glucose starvation condition, during which Ca^{2+} release through RyR2 was greater, AMPK was activated whereas mTOR was inactivated, as indicated by an increased level of phosphorylated AMPK and a reduced level of phosphorylated mTOR (Fig. 7A–7C). Importantly, knockdown of PKD2 with Ad-*PKD2*-shRNA1 (Fig. 7A–7C) and Ad-*PKD2*-shRNA2 (Supporting Information Fig. S1A, S1D, S1E) attenuated the glucose starvation-induced AMPK activation and mTOR inactivation.

Verification About the Role of PKD2 in Autophagy in H7-CMs

The role of PKD2 in autophagy was verified using another hESC line-derived cardiomyocytes, H7-CMs. H7-CMs were differentiated using a modified monolayer culture system that did not rely on the addition of either BMP-4 or activin-A [34]. Glucose starvation for 3 hours increased the LC3-II accumulation in H7-CMs (Supporting Information Fig. S6A, S6C). Glucose starvation also increased the expression of PKD2 proteins (Supporting Information Fig. S6A, S6B). Knockdown of PKD2 with Ad-*PKD2*-shRNA1 reduced the starvation-induced LC3-II accumulation (Supporting Information Fig. S6A, S6C). In the presence of 50 nM bafilomycin A1, Ad-*PKD2*-shRNA1 still markedly reduced the LC3-II accumulation under starvation (Supporting Information Fig. S6F, S6G). Furthermore, knockdown of PKD2 with Ad-*PKD2*-shRNA1 attenuated the starvation-induced AMPK activation and mTOR inactivation (Supporting Information Fig. S6A, S6D, S6E). As a control, Ad-*PKD2*-shRNA1 was found to effectively knockdown the expression of PKD2 in H7-CMs (Supporting Information Fig. S6A, S6B). These data from H7-CMs are similar to those obtained from HES2-CMs, supporting the notion that PKD2 promoted autophagic flux in hESC-CMs.

Discussion

The major findings of this study are as follows: (a) Glucose starvation caused an increased expression of PKD2 proteins in HES2-CMs. (b) Under glucose starvation, knockdown of PKD2 expression with two *PKD2*-shRNAs reduced autophagic flux in HES2-CMs, the effect of which persisted in the presence of bafilomycin A1. Conversely, overexpression of PKD2 promoted the autophagic flux in HES2-CMs. (c) *PKD2*-shRNAs aggravated the starvation-induced apoptotic cell death in HES2-CMs. (d) Knockdown of PKD2 reduced the caffeine-induced store Ca^{2+} release under glucose starvation. It also reduced the magnitude of spontaneous cytosolic Ca^{2+} oscillation and impaired the isoprenaline-stimulated cytosolic Ca^{2+} oscillation in HES2-CMs. Furthermore, co-immunoprecipitation and in situ proximity ligation assay demonstrated an increased physical interaction of PKD2 with RyR2 under glucose starvation. (e) *PKD2*-shRNAs substantially attenuated the starvation-induced AMPK activation and mTOR inactivation in HES2-CMs. (f) The effect of PKD2 knockdown on starvation-induced LC3-II accumulation, AMPK activation and mTOR inactivation were validated using another hESC-CM line H7-CMs. Taken together, the present study uncovered an important functional role of PKD2 in promoting autophagy and attenuating apoptotic death in hESC-CMs under glucose starvation. It is likely that, under glucose starvation, PKD2 interacts with RyR2 to modulate Ca^{2+} release from SR, promoting AMPK activation, and mTOR inactivation, consequently stimulating autophagic flux in HES2-CMs (Fig. 7D).

ADPKD is caused by loss-of function mutations in either PKD1 or PKD2. Recent studies have suggested a linkage between PKD1, autophagy and ADPKD progression. Knockout of PKD1 was found to impair autophagic flux and increase apoptosis in kidney cells, which may promote cyst formation in ADPKD patients [5–7]. However, there is still no report about the role of PKD2 in autophagy. In the present study, we used HES2-CMs to explore the potential role of PKD2 in autophagy. Glucose starvation was used to stimulate autophagy in HES2-CMs. The results showed that PKD2 knockdown by *PKD2*-shRNAs reduced the autophagic flux in HES2-CMs under glucose starvation, as demonstrated by reduced LC3-II accumulation in Western blots, which persisted in the presence of bafilomycin A1, and by decreased formation of autophagosome and autolysosome. Conversely, overexpression of PKD2 promoted the autophagic flux, as indicated by increased LC3-II accumulation as well as increased formation of autophagosome and autolysosome. In addition, *PKD2*-shRNAs increased apoptotic cell death under glucose starvation, as demonstrated by Western blot analysis of cleaved caspase 3 and TUNEL assay. The linkage between autophagy and apoptotic cell death of HES2-CMs was further confirmed by *Atg5*-siRNA study, in which suppression of autophagic flux by *Atg5*-siRNA increased apoptotic cell death. Together, these data suggest that PKD2 plays a critical role in promoting autophagic flux under glucose starvation, thereby protects cardiomyocytes from starvation (possibly ischemia)-induced cell death. Importantly, our data may have provided a possible mechanistic explanation for cardiomyopathy in ADPKD. We showed that PKD2 knockdown could impair cardiomyocyte autophagy even under 5.5 mM glucose concentration, which corresponds to the fasting blood glucose level. Therefore, it is conceivable that ADPKD patients may have an impaired autophagic flux in cardiomyocytes in their daily life, resulting in an increased apoptotic death of cardiomyocytes. Therefore, our present scheme of PKD2-autophagy-apoptosis may have important pathophysiological relevance in two distinct types of cardiomyopathy, namely (a) ADPKD, where PKD2 may be mutated, and (b) ischemic heart diseases, where there is low glucose supply.

Previous studies from other groups have demonstrated that PKD2 may interact with RyR2 to inhibit Ca^{2+} release from SR in cardiomyocytes, consequently elevating store Ca^{2+} content and increasing releasable Ca^{2+} during spontaneous Ca^{2+} oscillations and/or caffeine-induced Ca^{2+} transients [19]. In agreement with this notion, we found that PKD2 knockdown reduced the caffeine-induced Ca^{2+} release in HES2-CMs under glucose starvation (Fig. 5), and it also reduced the

overall amount of Ca^{2+} release during spontaneous Ca^{2+} oscillations and isoprenaline-induced Ca^{2+} oscillations (Supporting Information Figs. 3, 4). On the other hand, we also found that glucose starvation increased the amount of Ca^{2+} release during spontaneous Ca^{2+} oscillations and β-agonist (isoprenaline)-stimulated Ca^{2+} oscillations (Supporting Information Figs. 3, 4). Coincidently, co-immunoprecipitation and in situ proximity ligation assay demonstrated an increased physical interaction of PKD2 with RyR2 under glucose starvation. These data agree with the notion that, under glucose starvation condition, an increased interaction of PKD2 with RyR2 would elevate store Ca^{2+} content, resulting in more Ca^{2+} release during spontaneous Ca^{2+} oscillations and/or caffeine-induced Ca^{2+} transients. It is unclear how glucose starvation could cause an increased interaction of PKD2 with RyR2. However, PKD2 expression was found to be increased under glucose starvation (Fig. 1), which might be related to starvation-induced elevation of ER stress [35, 36]. One explanation is that the elevated PKD2 expression under starvation increased the number of PKD2 proteins that can interact with RyR2, resulting in more PKD2-RyR2 complex.

Ca^{2+} is an important second messenger that regulates autophagy [11, 12]. It is previously shown that intracellular Ca^{2+} release from through RyR could stimulate autophagy in several cell types including cardiomyocytes [12, 22, 37]. In the present study, we demonstrated that PKD2 may interact with RyR2 to modulate SR Ca^{2+} release. Therefore, it is conceivable that PKD2 may regulate autophagic flux via SR Ca^{2+} release. A possible scenario is that under glucose starvation condition, an increased amount of SR Ca^{2+} release during rhythmic Ca^{2+} oscillations and cardiomyocyte contractions would stimulate autophagic flux. On the other hand, knockdown of PKD2 may reduce the amount of SR Ca^{2+} release, thereafter decreases the autophagic flux under glucose starvation.

Mechanically, Ca^{2+} may act through multiple downstream targets including AMPK and mTOR to regulate autophagy [11, 12]. Therefore, we explored the possibility of whether PKD2 could modulate the activity of mTOR and/or AMPK. It is well documented that, under nutrient starvation condition, AMPK is activated while mTOR is inactivated, both of which promote autophagic flux [38, 39]. This was confirmed in HES2-CMs and H7-CMs (Fig. 7; Supporting Information Fig. S6). Importantly, *PKD2*-shRNAs substantially attenuated the starvation-induced AMPK activation and mTOR inactivation (Fig. 7; Supporting Information Fig. S6). Based on these, it is tempting to suggest that, at least under glucose starvation condition, PKD2 interacts with RyR2 to modulate Ca^{2+} release from SR, causing AMPK activation and mTOR inactivation, consequently stimulating autophagic flux, which serves to protect cardiomyocytes from apoptotic cell death.

Previously, PKD2 mutation mice have been used as an ADPKD model [19, 20]. Its limitation is that the contractile mechanisms of rodent heart differ considerably from that of human heart [40]. In the present study, we used hESC-CMs (HES2-CMs and H7-CMs) as ADPKD model, which offers a clear advantage over rodent cardiomyocytes. On the other hand, hESC-CMs are immature and they display fetal-like and sometimes embryonic-like structure and properties [41]. Therefore, caution has to be taken as to whether these results could also be applied to adult cardiomyocytes. As discussed above, our present scheme of PKD2-autophagy-apoptosis may be particularly relevant in ADPKD and ischemic heart diseases. In this regard, although the main clinical symptoms of ADPKD usually manifest at middle age, cardiac abnormality is also observed at early age [42, 43]. Ischemic heart diseases may also happen in some children/infants [44].

Conclusion

The present study demonstrates an important functional role of PKD2 in promoting autophagy and reducing apoptotic death in HES2-CMs under glucose starvation condition. The signaling axis may involve PKD2-RyR2-Ca^{2+}-AMPK-mTOR. We suggest that this scheme of PKD2-autophagy-apoptosis may have important pathophysiological relevance in ADPKD and ischemic heart diseases.

Acknowledgments

This work was supported by grants from National Natural Science Foundation of China 31470912, Hong Kong Research Grant Committee AoE/M-05/12, TBRS/T13–706/11, 14118516 and RGC-NSFC Joint Grant N_CUHK439/13.

Author Contributions

J.L.: conception and design, collection and/or assembly of data, data analysis and interpretation, manuscript writing; K.R.B. and L.J.: financial support; C.W.C., W.W.T., W.K., and E.N.Y.P.: collection and/or assembly of data; R.A.L.: financial support; X.Y.: conception and design, financial support, administrative support, data analysis and interpretation, manuscript writing, final approval of manuscript.

Disclosure of Potential Conflicts of Interest

The authors indicated no potential conflicts of interest.

References

1 Rangan GK, Tchan MC, Tong A et al. Recent advances in autosomal-dominant polycystic kidney disease. Intern Med J 2016; 46:883–892.

2 Chapman AB, Stepniakowski K, Rahbari-Oskoui F. Hypertension in autosomal dominant polycystic kidney disease. Adv Chronic Kidney Dis 2010;17:153–163.

3 Ecder T, Schrier RW. Hypertension in autosomal-dominant polycystic kidney disease: Early occurrence and unique aspects. J Am Soc Nephrol 2001;12:194–200.

4 Klionsky DJ, Emr SD. Autophagy as a regulated pathway of cellular degradation. Science 2000;290:1717–1721.

5 Zhu P, Sieben CJ, Xu X et al. Autophagy activators suppress cystogenesis in an autosomal dominant polycystic kidney disease model. Hum Mol Genet 2016;26:158–172.

6 Ravichandran K, Edelstein CL. Polycystic kidney disease: A case of suppressed autophagy? Semin Nephrol 2014;34:27–33.

7 Rowe I, Chiaravalli M, Mannella V et al. Defective glucose metabolism in polycystic kidney disease identifies a new therapeutic strategy. Nat Med 2013;19:488–493.

8 Tan VP, Miyamoto S. HK2/hexokinase-II integrates glycolysis and autophagy to confer cellular protection. Autophagy 2015;11:963–964.
9 Huang L, Dai K, Chen M et al. The AMPK agonist PT1 and mTOR inhibitor 3HOI-BA-01 protect cardiomyocytes after ischemia through induction of autophagy. J Cardiovasc Pharmacol Ther 2016;21:70–81.
10 Matsui Y, Takagi H, Qu X et al. Distinct roles of autophagy in the heart during ischemia and reperfusion: Roles of AMP-activated protein kinase and Beclin 1 in mediating autophagy. Circ Res 2007;100:914–922.
11 Parys JB, Decuypere JP, Bultynck G. Role of the inositol 1,4,5-trisphosphate receptor/Ca^{2+}-release channel in autophagy. Cell Commun Signal 2012;10:17.
12 East DA, Campanella M. Ca^{2+} in quality control: An unresolved riddle critical to autophagy and mitophagy. Autophagy 2013;9:1710–1719.
13 Hanaoka K, Qian F, Boletta A et al. Co-assembly of polycystin-1 and −2 produces unique cation-permeable currents. Nature 2000;408:990–994.
14 Shen PS, Yang X, DeCaen PG et al. The structure of the polycystic kidney disease channel PKD2 in lipid nanodiscs. Cell 2016;167:763–773. e711.
15 Venkatachalam K, Luo J, Montell C. Evolutionarily conserved, multitasking TRP channels: Lessons from worms and flies. Handb Exp Pharmacol 2014;223:937–962.
16 Venkatachalam K, Montell C. TRP channels. Annu Rev Biochem 2007;76:387–417.
17 Nauli SM, Alenghat FJ, Luo Y et al. Polycystins 1 and 2 mediate mechanosensation in the primary cilium of kidney cells. Nat Genet 2003;33:129–137.
18 Marx SO, Marks AR. Dysfunctional ryanodine receptors in the heart: New insights into complex cardiovascular diseases. J Mol Cell Cardiol 2013;58:225–231.
19 Anyatonwu GI, Estrada M, Tian X et al. Regulation of ryanodine receptor-dependent calcium signaling by polycystin-2. Proc Natl Acad Sci USA 2007;104:6454–6459.
20 Kuo IY, Kwaczala AT, Nguyen L et al. Decreased polycystin 2 expression alters calcium-contraction coupling and changes beta-adrenergic signaling pathways. Proc Natl Acad Sci USA 2014;111:16604–16609.
21 Paavola J, Schliffke S, Rossetti S et al. Polycystin-2 mutations lead to impaired calcium cycling in the heart and predispose to dilated cardiomyopathy. J Mol Cell Cardiol 2013;58:199–208.
22 Zou Y, Liang Y, Gong H et al. Ryanodine receptor type 2 is required for the development of pressure overload-induced cardiac hypertrophy. Hypertension 2011;58:1099–1110.
23 Abdul Kadir SH, Ali NN, Mioulane M et al. Embryonic stem cell-derived cardiomyocytes as a model to study fetal arrhythmia related to maternal disease. J Cell Mol Med 2009;13:3730–3741.
24 Wang Y, Li Z, Zhang P et al. Nitric oxide-cGMP-PKG pathway acts on orai1 to inhibit the hypertrophy of human embryonic stem cell-derived cardiomyocytes. Stem Cells 2015;33:2973–2984.
25 Luo J, Deng ZL, Luo X et al. A protocol for rapid generation of recombinant adenoviruses using the AdEasy system. Nat Protoc 2007;2:1236–1247.
26 Rotter D, Rothermel BA. Targets, trafficking, and timing of cardiac autophagy. Pharmacol Res 2012;66:494–504.
27 Mizushima N, Yoshimori T, Levine B. Methods in mammalian autophagy research. Cell 2010;140:313–326.
28 Kimura S, Noda T, Yoshimori T. Dissection of the autophagosome maturation process by a novel reporter protein, tandem fluorescent-tagged LC3. Autophagy 2007;3:452–460.
29 Sciarretta S, Zhai P, Shao D et al. Activation of NADPH oxidase 4 in the endoplasmic reticulum promotes cardiomyocyte autophagy and survival during energy stress through the protein kinase RNA-activated-like endoplasmic reticulum kinase/eukaryotic initiation factor 2alpha/activating transcription factor 4 pathway. Circ Res 2013;113:1253–1264.
30 Hariharan N, Maejima Y, Nakae J et al. Deacetylation of FoxO by Sirt1 plays an essential role in mediating starvation-induced autophagy in cardiac myocytes. Circ Res 2010;107:1470–1482.
31 Marambio P, Toro B, Sanhueza C et al. Glucose deprivation causes oxidative stress and stimulates aggresome formation and autophagy in cultured cardiac myocytes. Biochim Biophys Acta 2010;1802:509–518.
32 American Diabetes A. Diagnosis and classification of diabetes mellitus. Diabetes Care 2011;34: S62–S69.
33 Decuypere JP, Welkenhuyzen K, Luyten T et al. Ins(1,4,5)P3 receptor-mediated Ca^{2+} signaling and autophagy induction are interrelated. Autophagy 2011;7:1472–1489.
34 Bhattacharya S, Burridge PW, Kropp EM et al. High efficiency differentiation of human pluripotent stem cells to cardiomyocytes and characterization by flow cytometry. J Vis Exp 2014;52010.
35 de la Cadena SG, Hernandez-Fonseca K, Camacho-Arroyo I et al. Glucose deprivation induces reticulum stress by the PERK pathway and caspase-7- and calpain-mediated caspase-12 activation. Apoptosis 2014;19:414–427.
36 Yang J, Zheng W, Wang Q et al. Translational up-regulation of polycystic kidney disease protein PKD2 by endoplasmic reticulum stress. FASEB J 2013;27:4998–5009.
37 Chung KM, Jeong EJ, Park H et al. Mediation of autophagic cell death by type 3 ryanodine receptor (RyR3) in adult hippocampal neural stem cells. Front Cell Neurosci 2016;10:116.
38 Hardie DG, Ross FA, Hawley SA. AMPK: A nutrient and energy sensor that maintains energy homeostasis. Nat Rev Mol Cell Biol 2012;13:251–262.
39 Tan VP, Miyamoto S. Nutrient-sensing mTORC1: Integration of metabolic and autophagic signals. J Mol Cell Cardiol 2016;95:31–41.
40 Davis RP, van den Berg CW, Casini S et al. Pluripotent stem cell models of cardiac disease and their implication for drug discovery and development. Trends Mol Med 2011;17:475–484.
41 Keung W, Boheler KR, Li RA. Developmental cues for the maturation of metabolic, electrophysiological and calcium handling properties of human pluripotent stem cell-derived cardiomyocytes. Stem Cell Res Ther 2014;5:17.
42 Magnin-Verschelde S, Fichtner C, Lavocat MP et al. [Arterial hypertension with renal disease revealed by heart failure in infants: Two case reports]. Arch Pediatr 2012;19:501–505.
43 Lubrano R, Versacci P, Guido G et al. Might there be an association between polycystic kidney disease and noncompaction of the ventricular myocardium? Nephrol Dial Transplant 2009;24:3884–3886.
44 Barker DJ, Osmond C. Infant mortality, childhood nutrition, and ischaemic heart disease in England and Wales. Lancet 1986;1:1077–1081.


See www.StemCells.com for supporting information available online.